Crystal Plasticity Analysis of Scale Effect on Tensile Properties of Ferrite/Cementite Fine Lamellar Structure under Lattice Strain

YOHEI Yasuda[1, a *], TETSUYA Ohashi[1, b] and TAKURO Sugiyama[1,c]

[1]Department of Mechanical Engineering, Kitami Institute of Technology, Koencho 165, Kitami, Hokkaido 090-8507, Japan

[a]yasuda@newton.mech.kitami-it.ac.jp, [b]ohashi@newton.mech.kitami-it.ac.jp, [c]sugita@newton.mech.kitami-it.ac.jp

Keywords: Scale effect, Tensile properties, Fine lamellar structure, Lattice strain, Crystal plasticity analysis, Dislocations

Abstract. Tensile properties of ferrite lamella in pearlite under lattice strain are examined by a strain gradient crystal plasticity analysis. Tensile direction is made to be parallel to the lamella. Obtained results of macroscopic stress-strain relation of the lamella show significant increase of yield stress and strain hardening rate with the reduction of the lamella thickness and further increase of the yield stress with positive normal lattice strain parallel to the tensile direction in the ferrite layer. Whereas normal lattice strain perpendicular to the tensile direction contributes little to the tensile properties.

Introduction

Pearlite steels are widely used as structural materials such as cable wire of suspension bridge, railroad track and steel cord for tire because of their strong and ductile property. The property is affected a large degree by microstructure of pearlite. The microstructure is ferrite/cementite fine lamellar structures which are transformed from austenite. Flow stress of the pearlite increases with reduction of the lamella spacing due to strengthening of the ferrite layers by scale effect [1].

In our previous study [2], we showed a contribution of the strengthening of ferrite lamellae on the property of pearlite. It was found that the brittle cementite lamella could deform into plastic range if yield stress and strain hardening of the ferrite are sufficiently large, which we considered to take place from a scale effect. The scale effect on the mechanical properties of ferrite lamella in pearlite was examined quantitatively by a strain gradient plasticity analysis [3], while the effect of lattice misfit strain which is, for instance, formed during transformation from the austenite to the ferrite/cementite structure is left for further analysis. In this paper, we examine the scale effect on the tensile properties of the ferrite lamella in pearlite under lattice strain by the crystal plasticity analysis as a preliminary study on the effect of misfit strain.

Constitutive Equations for Crystal Plasticity Analysis

Analyses are made by using a crystal plasticity finite element method for body-centered cubic (bcc) crystal structures based on the analysis code CLP [4]. We assume that slip planes of the bcc crystal are {110}<111> and {112}<111>. For the convenience of the analysis, the Schmid's law is assumed for their activation.

We define the critical resolved shear stress $\theta^{(n)}$ on slip system *n* by the following equation,

$$\theta^{(n)} = \theta_0 + \sum_{m=1}^{24} \Omega^{(nm)} a \mu \tilde{b} \sqrt{\rho_S^{(m)}} + 3\beta \frac{\mu \tilde{b}}{d}, \tag{1}$$

where θ_0, μ, $\tilde{b}$, d and $\rho_S^{(m)}$ denote the lattice friction stress, the elastic shear modulus, magnitude of the Burgers vector, lamella thickness and the density of the statistically stored (SS) dislocations that accumulate on the slip system *m*. a and β are numerical coefficients. We employ $a = 0.1$ and

$\beta = 1$, respectively. $\Omega^{(nm)}$ is an interaction matrix. We use $\Omega^{(nm)} = 1$ for the diagonal components and $\Omega^{(nm)} \cong 1$ for the off-diagonal components.

Increment in the SS dislocation density on the slip system *n* is calculated by

$$d\rho_S^{(n)} = \left(\frac{c}{\tilde{b}L^{(n)}} - \frac{D}{\tilde{b}} \rho_S^{(n)} \right) d\gamma^{(n)}. \tag{2}$$

Here, $\gamma^{(n)}$ is the plastic shear strain of the slip system *n*. *c* and *D* are defined from a moving distance ratio of the edge and screw dislocations and a distance of the dislocation annihilation. We use $c = 1$ and assume $D = 2\tilde{b}$. $L^{(n)}$ is the mean free path of moving dislocations on the slip system *n* defined by the following model,

$$L^{(n)} = \mathrm{Min} \left[\frac{c^*}{\sqrt{\sum_m^{24} \varpi^{(nm)} \left(\rho_S^{(m)} + \left\| \rho_G^{(m)} \right\| \right)}}, d \right], \tag{3}$$

where c^* is a material constant and we assume $c^* = 10$. $\varpi^{(nm)}$ is a weighting matrix. We use $\varpi^{(nm)} = 0$ for the diagonal components and $\varpi^{(nm)} = 1$ for the off-diagonal components. $\left\| \rho_G^{(m)} \right\|$ is the density norm of the geometrically necessary (GN) dislocations on the slip system *m* [4].

Model and Boundary Condition of Numerical Analysis

Fig. 1(a) shows the pearlite model employed in this study. Shape of the entire model is a rectangle plate and it consists of three layers; a ferrite soft layer is sandwiched by two cementite hard layers. Dimension of the model is $l \times 3l \times 2l/15$ and thickness of the each layer is d (=l/3). We construct two models with d=125 and 500 nm and examine mechanical responses of the ferrite. The models are divided into eight-node finite elements. Total number of the elements for the model is 12288.

Material constants of the ferrite and cementite layer used in this study are shown in Table 1. Crystal orientations of the each layer are also shown in Fig. 1(a). Slip direction $[111]_\alpha$ and $[010]_\theta$ (index α and θ denote ferrite and cementite, respectively) are made to coincide with the *x* axis on

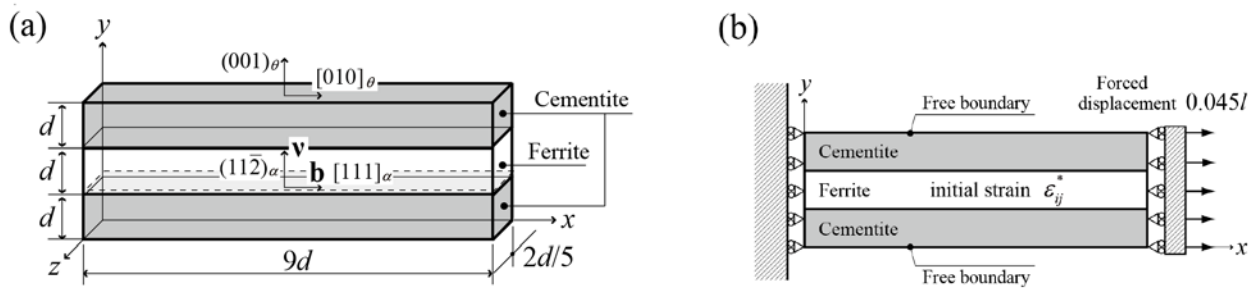

Fig. 1 (a) Pearlite model employed in this study and (b) boundary condition. **v** and **b** denote the slip plane normal vector and the slip direction vector.

Table 1. Material constants of ferrite and cementite.

		Ferrite	Cementite
Elastic compliance [Pa^{-1}]	s_{11}	7.54×10^{-12}	4.05×10^{-12}
	s_{12}	-2.77×10^{-12}	-1.28×10^{-12}
	s_{44}	8.62×10^{-12}	2.72×10^{-12}
Magnitude of Burgers vector [m]	b	2.48×10^{-10}	5.09×10^{-10}
Lattice friction [MPa]	θ_0	22.8	1.24×10^{3}
Initial SS dislocation density of *n* slip system [m^{-2}]	$\rho_S^{(n)}$	4.17×10^{9}	4.17×10^{10}

$(11\bar{2})_\alpha$ and at the same time $(001)_\theta$.

Fig. 1(b) shows boundary condition for the tensile deformation parallel to the layers. To study the scale effect under lattice strain, initial strain ε^*_{ij} consisting of a single component is added to the ferrite layer under the tying condition which keeps lateral surfaces at x=0 and x=9d as flat. The initial strains employed in this study are ε^*_{11}, ε^*_{22} and ε^*_{12} and the values are ε^*_{11}=ε^*_{22}=0.001 and ε^*_{12}=0.002. After that, a forced displacement of 0.045l is uniformly given to a lateral surface at x=9d and displacement of the opposite lateral surface is fixed in the direction parallel to the lamella. Other lateral surfaces are free boundaries.

Results and Discussion

Tensile properties of a ferrite lamella are evaluated by averaging the equivalent stress $\bar{\sigma}$ and strain $\bar{\varepsilon}$, where the averages are taken over the whole region of the ferrite layer. Fig. 2 shows the averaged equivalent stress-strain curves. Open and filled symbols represent results obtained when the lamella thickness d are 125 and 500 nm, respectively. Dashed lines indicate the onset of the plastic slip deformation in microscopic regions of the ferrite layer, which we call microscopic yield stress. The microscopic yield stress and strain hardening rate increase with a reduction of the lamella thickness. Main reason for the strengthening with the reduction of the thickness is the difficulty in dislocation emission from a dislocation source and the accumulation of the SS dislocations [3].

Furthermore, the microscopic yield stress of the model with normal lattice strain ε^*_{11} is larger than that of the model without lattice strain. On the other hand, normal lattice strain ε^*_{22} contributes little to the tensile property. Shear lattice strain ε^*_{12} lowers the microscopic yield stress but the stress-strain curve of the model with ε^*_{12} is almost the same as that of the model without lattice strain. Increase of the yield stress of the model with ε^*_{11} is equal to the residual stress and thereby the reason for the increase is an effect of the compressive residual stress parallel to the tensile direction.

Fig. 3 shows the average of accumulated SS dislocation density on active slip systems when the normal strain applied to the model is 1.5%. The slip system on which SS dislocation accumulates most is $(112)[11\bar{1}]$ for the models without the lattice strain and with ε^*_{22} and $(\bar{2}11)[\bar{1}11]$ and $(121)[1\bar{1}1]$ for the models with ε^*_{11} and ε^*_{12}. It turns out that the lattice strain ε^*_{11} and ε^*_{12} change the slip system on which SS dislocation accumulates most and the density of accumulated SS dislocation while the lattice strain ε^*_{22} doesn't change them.

Fig. 4 shows distributions of the equivalent stress $\bar{\sigma}$ after adding the lattice strain ε^*_{11} or ε^*_{12} to the model. Although the distribution after adding ε^*_{22} is not shown, the stress value is 0 in the whole

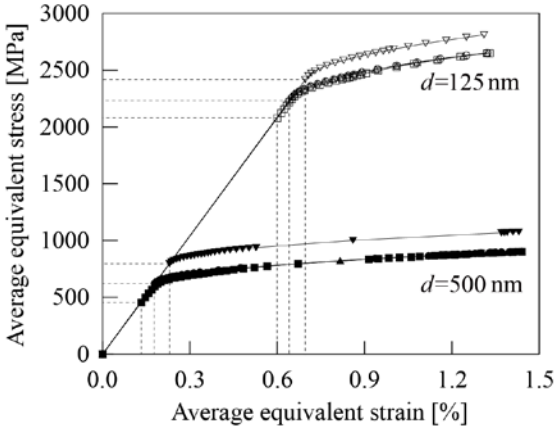

Fig. 2 Stress-strain response obtained for ferrite layer in pearlite when lamella thickness d is 125 and 500 nm. Symbols indicate ○; without lattice strain, ▽; with ε^*_{11}=0.001, △; with ε^*_{22}=0.001, □; with ε^*_{12}=0.002

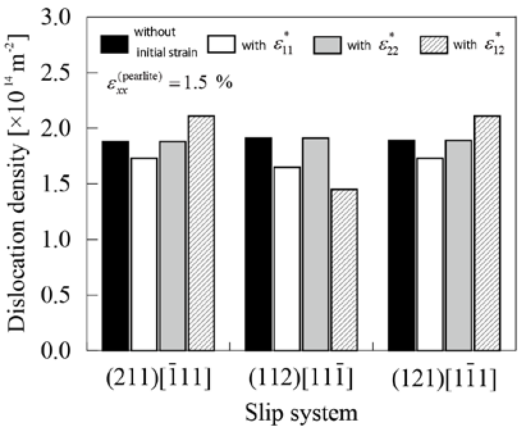

Fig. 3 Average of accumulated SS dislocation density on active slip systems obtained for ferrite layer in pearlite. Normal strain applied to the model is 1.5%. Lamella thickness d is 125 nm.

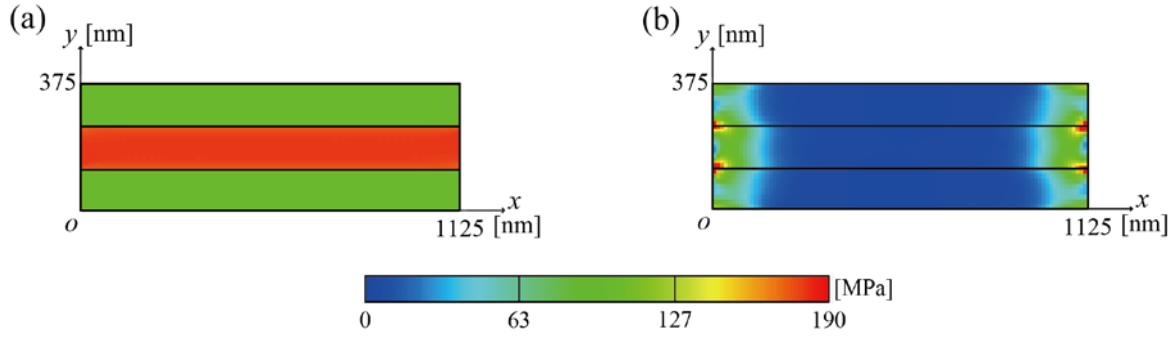

Fig. 4 Distributions of equivalent stress $\bar{\sigma}$ after adding lattice strain. The model with (a) normal lattice strain ε^*_{11} and (b) shear lattice strain ε^*_{12}.

region. While the distribution of equivalent stress in the model with ε^*_{11} is almost constant, the stress in the model with ε^*_{12} is concentrated at both lateral side and 0 in the remaining region. Therefore, the shear lattice strain ε^*_{12} only decreases the microscopic yield stress and slightly changes the stress-strain curve. Moreover, distributions of initial stresses are the reason for the change of the slip system on which SS dislocation accumulates most and the density of accumulated SS dislocation.

In this paper, plastic deformation of the cementite layer is not considered, whereas the cementite lamellae does deform plastically in pearlite microstructure [5]. Therefore, the numerical analysis considering the plastic deformation of cementite should be needed [6].

Summary

Tensile properties of ferrite lamella in pearlite under lattice strain were examined by a strain gradient crystal plasticity analysis. Obtained results are summarized as follows.

1. Yield stress and strain hardening rate increased with a reduction of lamella spacing.
2. Yield stress increased with positive normal lattice strain parallel to tensile direction.
3. Normal lattice strain perpendicular to tensile direction contributed little to tensile property.

Acknowledgement

This research was supported by Japan Science and Technology Agency (JST) under Collaborative Research Based on Industrial Demand “Heterogeneous Structure Control: Towards Innovative Development of Metallic Structural Materials”.

References

[1] X. Zhang, A. Godfrey, X. Huang, N. Hansen, Q. Liu, Microstructure and strengthening mechanisms in cold-drawn pearlitic steel wire, Acta Mater. 59 (2011) 3422-3430.
[2] T. Ohashi, L. Roslan, K. Takahashi, T. Shimokawa, M. Tanaka, K. Higashida, A multiscale approach for the deformation mechanism in pearlite microstructure: Numerical evaluation of elasto-plastic deformation in fine lamellar structures, Mater. Sci. Eng. A 588 (2013) 214-220.
[3] Y. Yasuda, T. Ohashi, to be submitted.
[4] T. Ohashi, R. Kondo, Evolution of dislocation patterns in a tricrystal model subjected to cycling loading, Phil. Mag. 93 (2013) 366-387.
[5] M. Tanaka, Y. Yoshimi, K. Higashida, T. Shimokawa, T. Ohashi, A multiscale approach for the deformation mechanism in pearlite microstructure: Experimental measurements of strain distribution using a novel technique of precision markers, Mater. Sci. Eng. A 590 (2014) 37-43.
[6] T. Shimokawa, T. Oguro, M. Tanaka, K. Higashida, T. Ohashi, A multiscale approach for the deformation mechanism in pearlite microstructure: Atomistic study of the rile of the heterointerface on ductility, Mater. Sci. Eng. A 598 (2014) 68-76.